Lab on a Chip



Cite this: Lab Chip, 2011, 11, 1464

www.rsc.org/loc PAPER

Capillary-driven automatic packaging†

Yuzhe Ding,‡a Lingfei Hong,‡b Baoqing Nie,a Kit S. Lama and Tingrui Pan*a

Received 20th December 2010, Accepted 10th February 2011 DOI: 10.1039/c0lc00710b

Packaging continues to be one of the most challenging steps in micro-nanofabrication, as many emerging techniques (e.g., soft lithography) are incompatible with the standard high-precision alignment and bonding equipment. In this paper, we present a simple-to-operate, easy-to-adapt packaging strategy, referred to as Capillary-driven Automatic Packaging (CAP), to achieve automatic packaging process, including the desired features of spontaneous alignment and bonding, wide applicability to various materials, potential scalability, and direct incorporation in the layout. Specifically, self-alignment and self-engagement of the CAP process induced by the interfacial capillary interactions between a liquid capillary bridge and the top and bottom substrates have been experimentally characterized and theoretically analyzed with scalable implications. High-precision alignment (of less than 10 μm) and outstanding bonding performance (up to 300 kPa) has been reliably obtained. In addition, a 3D microfluidic network, aligned and bonded by the CAP technique, has been devised to demonstrate the applicability of this facile yet robust packaging technique for emerging microfluidic and bioengineering applications.

Introduction

Packaging has always been a challenging step in microfabrication, as most microdevices incorporate more than one structural substrate.1 Specifically, bonding and alignment are two essential elements involved in any packaging process.2 Conventional bonding techniques, developed primarily for silicon-based semiconductor manufacturing, usually experience high temperatures (a few hundred to more than a thousand degrees), heavy mechanical loading (greater than one bar), and/ or strong electric fields (a few hundred to a few thousand volts across the interface), through which hermetic sealing of the device forms as necessary.3 Recently, polymeric materials have been extensively employed to build microengineered surfaces for a wide range of chemical and biological applications. However, packaging for emerging microfluidics and biomedical microdevices confronts completely different challenges, in which biocompatibility, bio-functionality, reversibility, thermal and chemical resistances, as well as macro-to-micro-interfaces preclude many of the traditional packaging processes from being used in traditional microelectronics. Therefore, surface chemical

In comparison with numerous studies on interfacial bonding, the capacity to align polymeric microstructures has neither been adequately researched nor addressed. In the conventional siliconbased processing, the mask aligner has still been held as the gold standard to provide high-accuracy and high-reliability alignment for multilayer packaging.² Whereas, several major issues, such as high-operation and maintenance costs, limited access, inflexible process flow, and restricted material selections, limit its potential application as the portfolio of new functional materials rapidly expands for micro-nanofabrication. For instance, large-scale microfluidic integration typically requires repetitive bonding and alignment steps of multilayer PDMS microstructures, ^{9,10} of which the packaging process has not been reliably established. Recently, several alternative alignment approaches have been proposed for multilayer microstructures, including the alignment key

modification serves as the primary route to join two bio-functional surfaces together, which relies on the formation of strong intermolecular interactions, e.g., covalent, electrostatic, or hydrogen bonds, between two sides, through intimate physical contact. For instance, polydimethylsiloxane (PDMS) has become the most popular material selection in polymeric microdevices for its excellent combination of mechanical (e.g., elastic and flexible), optical (e.g., transparent) and biological (e.g., biocompatible and non-toxic) properties, together with its low price and easy fabrication.5 The standard packaging techniques to seal microfabricated PDMS molds to various organic and inorganic substrates include oxygen plasma activation,6 organofunctional silane treatment,7 and step control of curing.8 Unfortunately, most of these are incompatible with existing highprecision alignment processes, leaving fabrication of 3D/multilayer PDMS microstructures difficult and unreliable.^{2,3}

^aMicro-Nano Innovations (MiNI) Laboratory, Biomedical Engineering, University of California, Davis, USA. E-mail: tingrui@ucdavis.edu

^bSchool of Instrumentation Science and Optoelectronics Engineering, Beihang University, Beijing, China

^eDepartment of Biochemistry and Molecular Medicine, Division of Hematology & Oncology, University of California, Davis, USA

[†] Electronic supplementary information (ESI) available: Calculation of the liquid film loading, a microscopic image of Vernier alignment markers, and a proposed CAP-enabled fabrication process for large-scale integrated microfluidics. See DOI: 10.1039/c0lc00710b ‡ Authors contributed equally.

structure,¹¹ the peg-in-hole interlocking mechanism¹² and the reversibly pluggable socket design.¹³ As a common feature in these dedicated designs, the geometric match of male and female components are necessary to facilitate structural engagement (*e.g.* matching pegs and holes, complementary fingers and sockets), from which different layers can be easily and quickly positioned and oriented with high reliability and repeatability.

On the other hand, capillary-driven self-assembly technique has been extensively explored to organize miniaturized objects automatically (from sub-micrometre to millimetre scales) into programmed 2D and 3D compartments. ^{14,15} In this process, the capillary force acts as the adhesive force on selective sites as well as the interactive guide to position and align the small objects spontaneously. To establish the confined region with capillary interactions, surface wettability patterning (hydrophobic *versus* hydrophilic areas) becomes necessary. ¹⁶ Although it has demonstrated use in self-organizing of millions of miniature components in parallel, to our best knowledge, this concept has yet to implement to align and package centimetre-scale substrates. ^{17,18}

In this paper, we present a simple-to-operate, easy-to-adapt packaging strategy, referred to as Capillary-driven Automatic Packaging (CAP), utilizing structurally directed capillary interactions to establish both bottom-to-top self-alignment and selfengagement in a single-step automatic process. Resembling to the well developed capillary-assisted self-assembly,17 the acting capillary interactions are enabled by an intermediate liquid layer confined in between two parallel surfaces with identical wetting boundaries, and position and orient the surfaces spontaneously.16 The structurally defined wetting boundaries have been both theoretically and experimentally investigated to achieve the optimal self-alignment performance as the capillary force increases linearly with the capillary length. Moreover, the capillary bridge formed between two surfaces results in elevated Laplace pressure (negative) for the surface self-engagement, ¹⁹ as the sandwiched liquid film gradually evaporates (and the film thickness reduces too). As a consequence, two surfaces are brought into intimate contact and form seamless joints through covalent bonding of pre-activated functional groups on surfaces. Unique advantages of CAP are summarized as follows: (1) the aligning and bonding can be achieved spontaneously through an evaporating capillary bridge in one single step; (2) the alignment structure can be incorporated in the same layer of the main structure (no additional layer or patterning is needed); (3) it can be adopted to multilayer microstructure assembly with high alignment resolution and excellent bonding performance; (4) the automatic packaging process can be potentially scaled up without using any dedicated fabrication equipment; (5) it can be applied to various new structural materials and unconventional fabrication techniques, as long as the bonding mechanism is compatible with the liquid capillary bridge; and (6) neither mechanical nor thermal treatment process is involved, which is desired in highly sensitive chemical and biological applications.

Concept

Capillary-driven automatic packaging (CAP) utilizes interfacial capillary interactions between the top and bottom surfaces and the intermediate liquid layer to establish both self-alignment

and self-engagement in the packaging process, extended from the basic principle of the capillary-driven self-assembly.¹⁷ Specifically, the capillary interactions include two force components, capillary force (F_C) along the wetting boundaries and suction force (F_S) from the negative Laplace pressure (ΔP) inside induced by liquid menisci.¹⁹ As illustrated in Fig. 1, the lateral component of the capillary force (F_C^{\perp}) attempts to spontaneously align the identical comb-shaped wetting patterns between two surfaces in order to minimize liquid surface energy. And the suction force together with the perpendicular component of the capillary force (F_C^{\parallel}) would gradually bring the surfaces into intimate contact, as the capillary bridge continuously evaporates. On contrary, presence of the gravitational force (G) of the substrate leads to potential misalignment as often the surface is not perfectly perpendicular to the gravitational plane. In order to maintain a negative adhesive pressure against the gravity on the moving part, a bottom-to-top self-alignment scheme of the CAP process is implemented, in which the capillary-suspended bottom substrate is gradually driven towards the fixed top surface, as evaporation continues. This is another clear distinction between the CAP process and the conventional packaging methods. In brief, the physical forces involved in the CAP process are the capillary force, the suction force and the gravitational force of the bottom substrate, as expressed in eqn (1), under the assumption that the alignment-related movement is relatively small, and therefore, the motion-induced friction is negligible 16,20

$$F_{\rm C} = \gamma D \tag{1a}$$

$$F_{\rm S} = \Delta P A = \frac{2\gamma \cos\theta}{h} A \tag{1b}$$

where the perimeter (*D*) and area (*A*) of the hydrophilic capillary region for self-alignment can be calculated as $D = L_o + 2nL_c$, and $A = L_o^2 + 4nwL_c$, accordingly (*n* is the number of the combshaped structures), as shown in Fig. 1. (L_c and *w* indicate the length and width of the combshaped alignment structures, respectively, and L_o is the length of the baseline structure. γ and θ indicate the surface tension and contact angle of the intermediate fluid, respectively, and *h* is the height of the capillary bridge.)

Self-alignment

As aforementioned, the lateral component of the capillary force (F_C^{\parallel}) is used to minimize the overall surface energy of the capillary fluidic layer and to position the top and bottom substrates through the identical comb-shaped wetting patterns for automatic alignment. As shown in eqn (1a), the strength of the capillary force is proportional to the length of the wetting boundary and the surface tension of the liquid. Therefore, adding

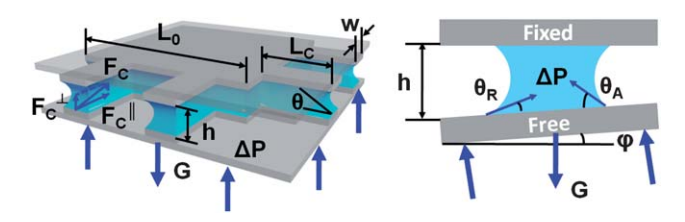


Fig. 1 Illustration of the principle of the capillary-driven automatic packaging (CAP).

or extending the comb-shaped microstructures (e.g., increasing n or $L_{\rm c}$) would extend the overall capillary force. In the case that the bottom surface is not completely perpendicular to the gravity, the parallel component to the surface would drag the substrate off from its aligned position, from which the force balance can be expressed as:

$$G\sin\varphi = F_{\rm C}(\cos\theta_{\rm R} - \cos\theta_{\rm A}) \tag{2a}$$

where φ is the tilting angle of the bottom substrate, θ_A and θ_R represent the advancing and receding contact angles of the menisci, respectively. As a consequence, the misalignment (Δx) between two substrates can be quantitatively calculated as:

$$\Delta x = h(\sin\theta_{A} - \sin\theta_{R})/(\cos\theta_{A} - \cos\theta_{R})$$

$$= (G/F_{C}) \left(h\sin\varphi/2\sin\left(\frac{\theta_{A} + \theta_{R}}{2}\right) \right)$$
 (2b)

Self-engagement

Self-engagement simply relies on the suction pressure from the intermediate liquid layer as shown in eqn (1b). As liquid in the capillary bridge continues evaporating, its height gradually reduces and the negative pressure rises inside as predicted by Laplace equation. As previously reported, the pressure inside capillary bridges can be as high as -17 bar, which provides significant and uniform lifting (hydrostatic nature) force for the bottom substrate to establish close physical contact with the top for the subsequent covalent bonding between two functionalized surfaces. Eqn (3) shows the relationship among the three related forces:

$$G\cos\varphi \le 2F_{\rm C}(\sin\theta_{\rm A} + \sin\theta_{\rm R}) + F_{\rm S}$$
 (3)

It is worth noting that the Laplace pressure inside the capillary bridge drives the bottom substrate towards the fixed top surface, which can be considerably greater than the gravitational force.

Experimental methods

Microfabrication

In the proof-of-concept work, we have demonstrated the widely adaptable capillary-driven automatic packaging (CAP) process on PDMS-based microdevices due to their dominant popularity in biological and chemical applications. 1,22,23 Specifically, the fabrication process involves both replica molding (soft lithography) of PDMS and micropatterning (photolithography) of a photodefinable dry-film resist. The dry-film resist is selected for its easy processability and mechanical flexibility as a master mold. Moreover, it can be bonded to PDMS through plasma-activated hydroxyl groups as a structural through-layer for 3D microfluidics, which is compatible with the CAP process. The detailed process flow of dry-film photopatterning and PDMS molding is summarized as follows:

Dry-film micropatterning. Dry-film resist (PerMx 3000, DuPont) has been introduced by our group previously as both molding and structural materials in microfabrication for its direct processability, mechanical flexibility, chemical resistivity, high resolution, as well as optical clarity.^{3,12,13,24} The dry-film layer with

a nominal thickness of 50 μm is first laminated onto a planar polymer support (Mylar, DuPont) at 65 °C with a moderate pressure of 400 kPa. Subsequently, the dry-film layer is UV-exposed through a photomask in a proximity mode at the exposure energy of 600 mJ cm⁻², followed by an immediate post-exposure bake at 115 °C for 3 minutes (Fig. 2a). And the exposed dry film is then developed in an ultrasonic bath with propylene glycol monomethyl ether acetate (PGMEA) for 2 minutes, followed by an isopropyl alcohol (IPA) rinsing step to remove the organic residual from the film. The micropatterned dry-film layer can be directly used as a master for PDMS replica molding or detached from the support as a structural layer for polymeric microdevices.

PDMS replica molding. PDMS pre-polymer, a mixture of a base and a curing agent at 10:1 weight ratio (SYLGARD 184, Dow Corning), is poured and thermally cured on a micropatterned dry-film mold at 80 °C for 2 hours, followed by gently peeling off the Mylar substrates without damaging the dry-film mold, as illustrated in Fig. 2b.

Packaging

The first step of the CAP process is to create geometrically defined capillary region on the polymeric substrates. Surface modification becomes necessary to introduce hydroxyl groups on both the top and bottom surfaces, which can be either achieved by wet chemical or dry physical treatment.^{7,25,26} In this case, wettability contrast of capillary region is defined by selective oxygen plasma treatment (at 90 W for 30 s) through a shadow mask made of dry film. According to our previous investigation, the shadow mask made of dry film photoresist provides moderate adhesion to both soft (e.g., PDMS) and rigid substrates (e.g. glass slides and Petri dishes).¹² After peeling the chip off from the mold, the hydrophilic regions on PDMS are present on the uncovered surface while the intrinsic hydrophobicity retains in the molded areas in Fig. 2c. Contact angles of the hydrophilic and hydrophobic regions have been measured for the characterization of the wettability

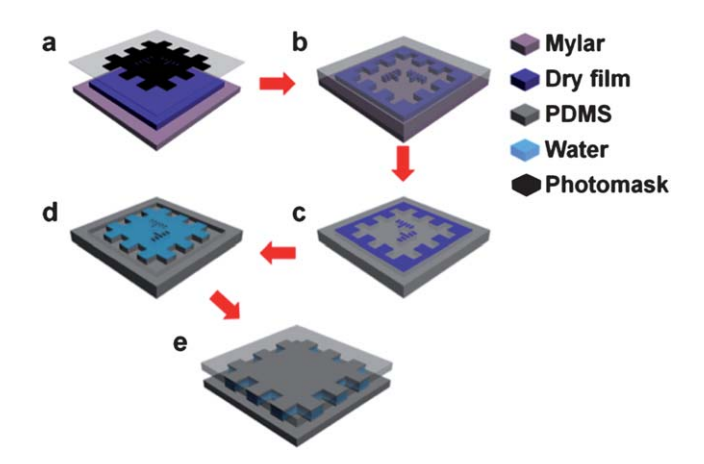


Fig. 2 Illustration of the CAP-enabled microdevice fabrication process, including (a) micropatterning of a shadow mask made of dry film, (b) PDMS replica molding, (c) selective oxygen plasma treatment through the shadow mask, (d) DI water loading in the defined hydrophilic regions, and finally (e) self-alignment and self-engagement steps between two chips with identical capillary alignment patterns.

contrast.²⁷ Secondly, the molded PDMS substrates with defined wettability contrast are loaded with DI water. A thin layer of water film of about 200 µm in thickness (calculated based on eqn S1 in the ESI†) is expected to retain on the hydrophilic areas of substrates (Fig. 2d), according to the wetting theory.²⁸ The top substrate is then fixed to a horizontal plane, to which the bottom one subsequently sticks *via* an automatically formed capillary bridge, as shown in Fig. 2e. The pre-aligned sandwiched microstructures are held suspended over a hotplate at 90 °C or in a vacuum desiccator to accelerate the evaporation process of the intermediate capillary layer, which carries out the self-alignment and self-engagement steps simultaneously.

Characterization

Characterization of self-alignment. Built-in Vernier alignment markers (as shown in Fig. S1, ESI \dagger) are included in the device layout to calibrate the precision of the alignment process. A differential grid of Vernier alignment markers allows measurement of minimal misalignment of 5 μ m. The structural misalignment can be easily assessed using a standard microscope after the CAP process.

Characterization of bonding strength. Standard blister test has been applied to evaluate the bonding strength between two substrates^{29,30} through the CAP process or using the classic oxygen plasma bonding with direct contact. A fluidic reservoir of 5 mm in diameter and 50 μm in height is incorporated within one substrate prior to the plasma-activated bonding. A through-hole is punctured by a blunt needle (14 gauge, i.e., 2.1 mm in outer diameter, 1.6 mm in inner diameter) for external micro-tube connection. Silicone micro-tubing is inserted in the through-hole and sealed by additional PDMS pre-polymer after the CAP process or oxygen plasma bonding. To evaluate the bonding strength, a programmable syringe pump is used to controllably inject DI water into the PDMS chamber, while a digitally recordable pressure sensor (PX26, Omega) continuously monitors the hydraulic pressure inside. At the leakage point, a drastic release of pressure can be observed in the recorded pressure curve. Eight identical devices for the CAP process and four indistinguishable samples for the oxygen plasma bonding are fabricated and tested for the bonding strength, respectively.

Results and discussion

Self-alignment

(a) Influence of capillary force. As aforementioned, capillary force plays a dominant role in the self-alignment of the CAP process, which is proportional to the length of the wetting boundary of the capillary region (eqn (1a)). As shown in Fig. 1, the periodic comb-shaped microstructures have been attached to the capillary region to extend the linear border and thus the capillary force. The self-alignment resolution has been experimentally evaluated at various lengths of capillary boundary, arranging from 1 to 6 times of that of the baseline (L_o), in which the weight of the bottom substrate is kept at the same level. Fig. 3a summarizes the measurement results in comparison with the theoretical analysis using various lengths of wettability-defined capillary boundary. According to the model developed in

the Concept section (eqn (2b)), the overall misalignment is inversely proportional to the length of capillary boundary (D). As can be seen, the experimental data are in good agreement with the modeled results, in which a decreasing tendency of the misalignment has been observed as the capillary boundary length rises. As expected, the minimum misalignment of $8.0 \pm 2.5 \, \mu m$ is achieved at the longest capillary boundary, which is 6 times of the baseline ($6L_o$). Further increment of the capillary length would continuously reduce misalignment at the expense of substantially expanded dimensions of the devices. It is worth noting that w cannot be considerably reduced due to Rayleigh instability.³¹

(b) Influence of gravitational force. Gravitational force of the suspended bottom substrate is the main cause of the misalignment as illustrated in the Concept section (eqn (2a)). Alignment performance of substrates with various weights has also been characterized experimentally for influence of the gravitational force, of which the ratio of weight to capillary force ranges from 0.32 to 2.56. Fig. 3b compares the experimental measurement with theoretical predication according to eqn (2b). As expected, the misalignment grows linearly with increasing substrate weight. Further weight increment could result in failure of capillary

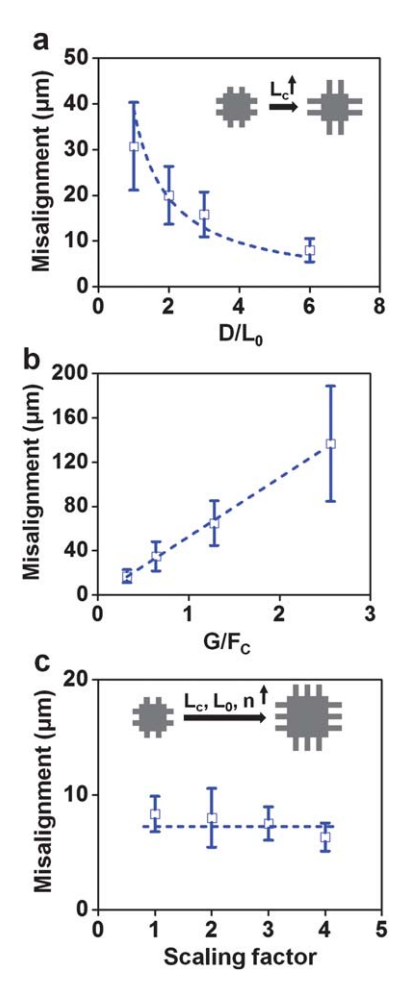


Fig. 3 Characterization of self-alignment performance with key design parameters: (a) the length of the capillary boundary, (b) the gravitational force of the suspended bottom substrate, and (c) the isometric scaling (for the scaling factor of 1, L_c is 1.25 mm, L_o is 0.5 cm, and n is 5, given the substrate thickness is fixed).

suction for the self-engagement step and leave the self-alignment process unreliable.

(c) Scalability of self-alignment. One important feature of the CAP process is the potential scalability. Among all three related physical forces, suction and gravitational forces are proportional to the surface area, given the thickness of the substrate is fixed (normally it is the case in most microdevices). As shown in eqn (1), the capillary force (F_C) is proportional to the perimeter of the hydrophilic region, in which the product of n and L_c plays a dominant role. If n and L_c in the design are both scaled with the characteristic length, the capillary force can be approximated as a linear function of the surface area as well. This would lead to that all three force components obey the same scaling law. According to our model (eqn (2b)), the misalignment is proportional to the ratio of the gravitational force to the capillary force. Therefore, this indicates that the structural misalignment is only related to the thickness and wettability of the sandwiched capillary bridge, which will not be affected by isometric scaling. Fig. 3c summarizes alignment performance of the substrates with various length scales experimentally, of which the scaling factor ranges from 1 to 4, which basically proves the scalable design of the CAP method. In general, extending the concept to align substrates with relative large surface area (e.g., the standard 4 inch substrates) is potentially feasible. Further upscaling would encounter the instability of elongated capillary bridges in the comb-shaped microstructures (i.e., Rayleigh instability), 31 undesired mechanical bending of soft substrates, 32 and non-uniform evaporation process, all of which would work against the alignment precision and bonding uniformity.

Self-engagement and automatic bonding

In the proof-of-concept study, we have demonstrated the CAP concept on the widely used PDMS microstructures. The micromolded PDMS surfaces are selectively activated with hydroxyl groups through dry-film shadow masks for capillary formation (with the water contact angle of $4.7 \pm 1.2^{\circ}$, in contrast to that of intrinsic PDMS, $88.9 \pm 1.5^{\circ})^{27,33}$ and subsequently covalent chemical bonding. Following evaporation of capillary bridge, bonding happens spontaneously upon physical contact between the two pre-activated substrates. The standard blister test has been carried out to evaluate the bonding strength of the PDMS-PDMS interface. As summarized in Fig. 4, the average bonding strength of 247.1 kPa (± 39.5 kPa) is found comparable to that of the plasmaactivated PDMS bonding with direct contact, from which 271.1 kPa (±77.8 kPa) is obtained.30 Therefore, the capillary bridge formed during the CAP process can retain the functionality of hydroxyl groups for following covalent bond without any additional treatment. This desired feature allows the CAP approach to be extended to a broader category of new inorganic and organic structural materials and emerging micro-nanofabrication techniques as long as the bonding mechanism is compatible with the liquid capillary bridge. For instance, it can be easily extended to packaging of classic multilayer PDMS microstructures, e.g. largescale integrated microfluidics (a dedicated CAP-enabled process flow is proposed for those 3D microstructures in Fig. S2 of ESI†).9,10 Besides the demonstrated applicability on PDMS and dry-film substrates, for instance, the inorganic surfaces, like the

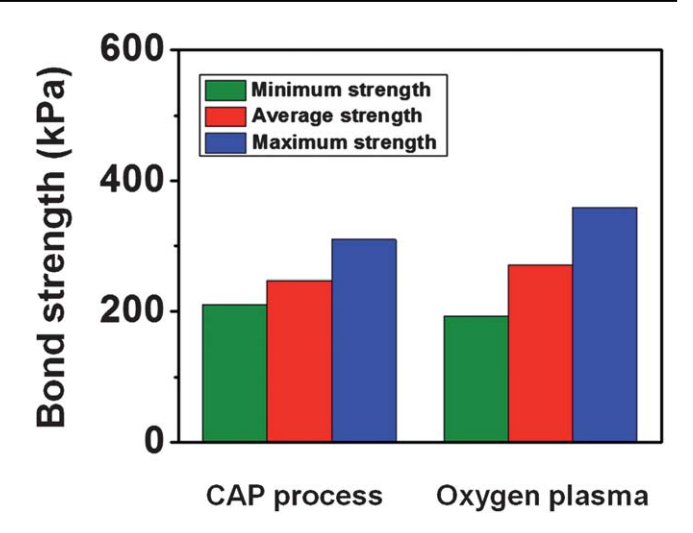


Fig. 4 Characterization of the bonding strength in the capillary-driven automatic packaging.

micropatterned silicon wafers and glass substrates, can be selectively activated by the oxygen plasma treatment or wet chemistry through photoresist micropatterns.33 Following formation of a sandwiched capillary bridge between silicon and glass substrates, a low temperature annealing (less than 100 °C) would be compatible with self-engagement of the CAP process to establish Si-O-Si bonds.34,35 Another example using organic substrates could be fabrication of polyethylene terephthalate-based (PET) microfluidic chips. Laser-micromachined PET substrates can be plasma-activated and subsequently bonded through C-O-C covalent bond.³⁶ This is essentially a similar case as the PDMS-PDMS packaging. In summary, the CAP approach can be directly extended to a wide range of functional materials and unconventional fabrication processes, a highly desired feature for rapidgrowing bioengineering and microfluidic applications. General guideline for the CAP compatible substrates only requires (a) patternable surface wettability (either chemical or physical), and (b) bonding can happen upon physical contact once the capillary bridge is eliminated.

Demonstration of the multilayer CAP process for 3D microfluidic devices

The CAP approach can be of extensive use in constructing 3D microfluidic devices, of which the multilayer alignment is typically challenging and unreliable. Fig. 5 presents a prototype of 3D microfluidic networks, aligned and sealed using the CAP process, consist of four sets of microchannels filled with different colored solutions. Both the top and bottom microchannels are fabricated by PDMS replica molding and connected through a through-hole layer made of the plasma-activated photopatterned dry-film resist. Alignment between top and middle or between middle and bottom substrates is achieved through the capillary bridge formation confined in the hydrophilic regions accordingly. As can be seen, the identical comb-shaped micropatterns through each layer guide the multilayer self-packaging process with precise alignment and uniform bonding. The resulted 3D microstructures enable the spatially crossover microflow patterns.

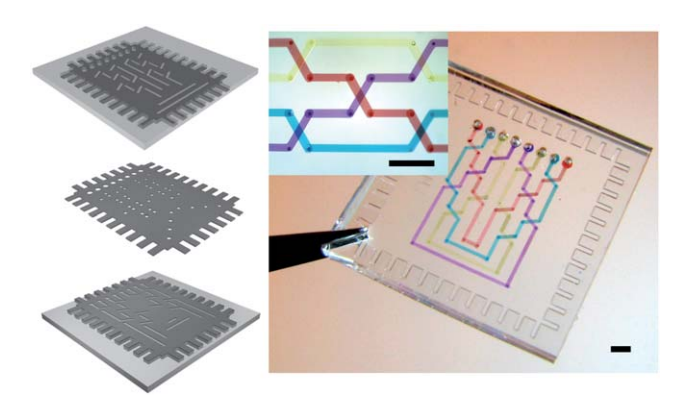


Fig. 5 3D microfluidic networks aligned and sealed using the CAP process (scale bar: 1 mm).

Conclusion

In this paper, we have developed a universal self-packaging technique, referred to as Capillary-driven Automatic Packaging (CAP) that utilizes the interfacial capillary interactions to establish both bottom-to-top self-alignment and self-engagement in a single-step process. In particular, the CAP technique has several unique features, including (a) the high-resolution selfalignment (less than 10 µm) of centimetre-scale chips achieved by the extended capillary length of the comb-shaped borders; (b) excellent self-engagement and bonding performance (up to 300 kPa); (c) the capacity of multilayer microstructure assembly; (d) wide adaptability to various structural materials; (e) spontaneous processing without using any dedicated equipment; and (f) neither thermal nor mechanical treatment involved. Applicability of the CAP technique has been demonstrated by a 3D microfluidic device with complex crossover microflow patterns. In summary, the novel CAP technique enables high-alignment resolution and automatic loading for packaging of various substrates and surfaces, which can be widely employed in microdevices for point-of-care diagnosis, controlled drug delivery, and combinatorial biological screening.

Acknowledgements

This work is in part supported by the National Science Foundation CAREER Program (ECCS-0846502). The authors would like to acknowledge DuPont Company for generously providing PerMX dry-film samples. LH and BN acknowledge the graduate fellowship support from China Scholar Council.

References

1 J. Cha, J. Kim, S.-K. Ryu, J. Park, Y. Jeong, S. Park, S. Park, H. C. Kim and K. Chun, J. Micromech. Microeng., 2006, 16, 1778-

- 2 J. Kim, J. Baek, K. Lee and S. Lee, Sens. Actuators, A, 2005, 119, 593-
- 3 W. Wei and T. Pan, Ann. Biomed. Eng., 2011, 39, 600-620.
- 4 Y. P. Zhao, L. S. Wang and T. X. Yu, J. Adhes. Sci. Technol., 2003, **17**, 519–546.
- 5 Y. Xia and G. M. Whitesides, Angew. Chem., Int. Ed., 1998, 37, 550-575
- 6 D. C. Duffy, O. J. A. Schueller, S. T. Brittain and G. M. Whitesides, J. Micromech. Microeng., 1999, 9, 211–217.
- 7 L. Tang and N. Y. Lee, Lab Chip, 2010, 10, 1274-1280.
- 8 M. A. Eddings and B. K. Gale, J. Micromech. Microeng., 2006, 16, 2396-2402.
- 9 M. A. Unger, H.-P. Chou, T. Thorsen, A. Scherer and S. R. Quake, Science, 2000, 288, 113-116.
- 10 T. Thorsen, S. J. Maerkl and S. R. Quake, Science, 2002, 298, 580-
- 11 B.-H. Jo, L. M. V. Lerberghe, K. M. Motsegood and D. J. Beebe, J. Microelectromech. Syst., 2000, 9, 76-81.
- 12 S. Zhao, A. Chen, A. Revzin and T. Pan, Lab Chip, 2011, 11, 224–230.
- 13 A. Chen and T. Pan, Lab Chip, 2011, 11, 727-732.
- 14 K. F. Bohringer, J. Micromech. Microeng., 2003, 13, S1-S10.
- 15 N. Bowden, F. Arias, T. Deng and G. M. Whitesides, Langmuir, 2001, 17, 1757–1765.
- 16 U. Srinivasan, D. Liepmann and R. T. Howe, J. Microelectromech. Syst., 2001, 10, 17-24.
- 17 N. Bowden, A. Terfort, J. Carbeck and G. M. Whitesides, Science, 1997, **276**, 233-235
- 18 N. Bowden, S. R. J. Oliver and G. M. Whitesides, J. Phys. Chem. B. 2000, **104**, 2714–2724.
- 19 A. Gerlach, H. Lambach and D. Seidel, Microsyst. Technol., 1999, 6, 19-22
- 20 B. J. Choi, M. Meisel, M. Colburn, T. B. Bailey, P. Ruchhoeft, S. V. Sreenivasan, F. Prins, S. Banerjee, J. G. Ekerdt and C. G. Willson, Proc. SPIE-Int. Soc. Opt. Eng., 2001, 4343, 436-442.
- 21 P. Mela, N. R. Tas, T. Kramer, J. W. Berenschot and A. van den Berg, Nano Lett., 2003, 3, 1537-1540.
- 22 G. M. Whitesides, Nature, 2006, 442, 368-373.
- 23 X. Y. Jiang, S. Takayama, X. P. Qian, E. Ostuni, H. K. Wu, N. Bowden, P. LeDuc, D. E. Ingber and G. M. Whitesides, Langmuir, 2002, 18, 3273-3280.
- 24 S. Zhao, H. Cong and T. Pan, Lab Chip, 2009, 9, 1128-1132.
- 25 K. S. Lee and R. J. Ram, Lab Chip, 2009, 9, 1618-1624.
- 26 D. C. Duffy, J. C. McDonald, O. J. A. Schueller and G. M. Whitesides, Anal. Chem., 1998, 70, 4974-4984.
- 27 S. Bhattacharya, A. Datta, J. M. Berg and S. Gangopadhyay, J. Microelectromech. Syst., 2005, 14, 590-597.
- 28 P. G. de Gennes, F. B. Wyart and D. Quere, Capillarity and Wetting Phenomena: Drops, Bubbles, Pearls, Waves, Springer, New York,
- 29 A. Sofla, E. Seker, J. P. Landers and M. R. Begley, J. Appl. Mech., 2010, 77, 031007.
- 30 M. A. Eddings, M. A. Johnson and B. K. Gale, J. Micromech. Microeng., 2008, 18, 067001.
- 31 T. R. Powers and R. E. Goldstein, Phys. Rev. Lett., 1997, 78, 2555-2558
- 32 J. H. Tong, C. A. Simmons and Y. Sun, J. Micromech. Microeng., 2008, 18, 037004.
- 33 D. Bodas and C. Khanmalek, Microelectron. Eng., 2006, 83, 1277-1279
- 34 T. Suni, K. Henttinen, I. Suni and J. Mäkinen, J. Electrochem. Soc., 2002, 149, G348-G651.
- M. M. R. Howlader, S. Suehara, H. Takagi, T. H. Kim, R. Maeda and T. Suga, IEEE Trans. Adv. Packag., 2006, 29, 448-456.
- Z. Wu, N. Xanthopoulos, F. Reymond, J. S. Rossier and H. H. Girault, Electrophoresis, 2002, 23, 782-790.